



# Analysis of Large-Scale In Situ Shear Tests of Sandy Gravel with Cobbles

Junwei Jin<sup>1</sup> · Qianqian Jin<sup>1</sup> · Mingyu Li<sup>1</sup> · Bo Liu<sup>2</sup> · Shiyong Zhao<sup>3</sup> · Yanqing Wei<sup>4</sup>

Received: 25 May 2023 / Revised: 19 February 2024 / Accepted: 20 March 2024  
© The Author(s), under exclusive licence to the Iran University of Science and Technology 2024

## Abstract

Shear strength of sandy gravel with cobbles is difficult to determine for usually an in situ test needs to be performed. Six group of in situ tests were conducted to investigate the shear strength of sandy gravel with cobbles. However, the inner friction angle was highly underestimated compared with those from the other methods. This failure result could be explained comprehensively. The strength parameters were also investigated using a DCP test, an experimental method and a theoretical method. Moreover, a numerical simulation method was also used to determine the failure mode of the in situ test. Through comprehensive comparison of these results, the soil failure mechanism in the tests did not follow the direct shear failure but did follow the bearing-capacity failure model. The bottom boundary could not provide enough capacity during the test; hence, the shear strength was underestimated. Moreover, the in situ test results could be explained through the Meyerhof bearing-capacity theory on shallow foundations subjected to inclined loads. With increasing normal load, the horizontal force decreased, resulting in a small inner-friction angle. The theoretical result of the inner-friction angle of sandy gravel with cobbles was  $42 \sim 47.5^\circ$  in these test, which coincided with the numerical simulation and empirical methods.

**Keywords** Large-scale in situ direct shear test · Shear strength · Bearing capacity failure · Sandy gravel with cobbles · Numerical simulation

---

✉ Mingyu Li  
mingyu\_li@zzu.edu.cn

Junwei Jin  
jinjunwei@zzu.edu.cn

Qianqian Jin  
jinqianqian@gs.zzu.edu.cn

Bo Liu  
bo-robert.liu@polyu.edu.hk

Shiyong Zhao  
zsy18039516165@163.com

Yanqing Wei  
wyq1987@lit.edu.cn

- <sup>1</sup> School of Civil Engineering, Zhengzhou University, No. 100 Kexue Road, Zhengzhou, China
- <sup>2</sup> School of Civil and Environmental Engineering, Hong Kong Polytechnic University, No. 11 Yucai Road, Hong Kong, China
- <sup>3</sup> Urban Rail Transit Engineering Company Limited of China Railway 15th Bureau, No. 6 Changluo Road, Luoyang, China
- <sup>4</sup> School of Civil Engineering, Luoyang Institute of Science and Technology, No. 90 Wangcheng Road, Luoyang, China

## List of Symbols

$N$	The normal force
$F$	The horizontal force
$A$	The section area of the shear box
$h$	The distance from the horizontal force to the ground
$\sigma$	The normal stress
$\tau$	The shear stress;
$c$	The cohesion
$\phi$	The internal friction angle
$d_{10}$	The particle size for 10% of the soil particles a finer
$d_{30}$	The particle size for 30% of the soil particles a finer
$d_{60}$	The particle size for 60% of the soil particles a finer
$C_c$	The coefficient of grading
$C_u$	The coefficient of uniformity
$N_b, N_d,$ and	The bearing-capacity coefficients of the foundation
$N_c$	
$B$	The width of the base

$c_k$	The standard value of cohesion (kPa) in the range of one times the width of the short side of the foundation
$N_{120}$	The number of drops in the dynamic cone penetration test
$\xi_c$ , $\xi_b$ , and $\xi_c$	The shape coefficients of the foundation
$f_{uk}$	The standard value of the bearing capacity of the foundation
$\theta$	The angle between the combined force R and vertical axis
$B$	The plate width, 0.5 m in this test
$L$	The plate length
$D$	The plate depth
$B'$	The effective plate width

## 1 Introduction

Gravel or cobble mixtures are commonly encountered in geotechnical projects, such as slopes, foundations, and tunnels [1, 2]. For stability analysis, it is critical to determine the shear strength parameters of the materials, namely, cohesion and friction angle.

The direct shear test was first used by Coulomb in 1991 [3], and it has been widely used to estimate the strength parameters of soils. Although the direct shear test has limitations compared to the tri-axial test, it is still prevalent in practise [4–7]. This method has been included in test standards in almost every country [8, 9]. The scale of the shear box must be large enough compared to the size of the soil particles to obtain reliable shear behaviour [10]. The Department of Transport and Main Roads, Queensland, suggested that the shear box should be no less than 300 mm in width or ten times the maximum particle size for coarse-grained granular materials. After consolidation, the sample thickness should not be less than 120 mm or six times the maximum particle size [11]. The testing of coarse soils for shear strength could be problematic, particularly for cobbles with more than 20 larger sized particles because most laboratory testing equipment is used for small-sized samples (relative to the size of soil particles) [12]. Researchers have used a large shear box in the laboratory to study the interface shear strength of sub-ballast reinforced with different types of geomembranes and geogrids [13]. The remoulded frozen soil samples under frozen, transition, freeze–thaw conditions were analysed [14], and large-scale cyclic simple shear tests and post-cyclic monotonic simple shear tests were performed on the gravelly soils [15].

In many cases, it is not practical or possible to use such large nondisturbed samples in the laboratory for testing, especially for noncohesive materials [16]. An in situ direct shear test was performed by horizontally pulling a latticed shearing frame embedded in the ground under a constant vertical load on the sample [17]. The method has been used successfully for testing rockfills, sands, and clays. A case study used the simplified large in situ direct shear test to determine the shear strength of roller compacted rockfills. The shear strength of roller compacted rockfill could be derived directly using the Mohr–Coulomb criterion [18]. A large-scale direct shear test of a soil–rock mixture was performed, and a digital image process was used to obtain the proportion and distribution of the rock blocks [19]. The ratio of rock particles controlled the deformation and fracture mechanism of soil–rock mixtures.

During the construction of subways in Luoyang city, deep excavations were needed for the subway stations. Sandy gravels with cobbles were encountered during the process. Six large in situ direct shear tests were carried out at one of the sites to determine the shear strength parameters of the sandy gravel with cobble. The test method followed the recommended guidelines in the Chinese Code, and this method is also commonly used to measure in situ rock strength according to ASTM. Through the analysis of the test results, the friction angle obtained via shear tests was nearly half that obtained via empirical methods and reported in the literature. To explain why the in situ direct shear test underestimates the strength of the soil, a finite difference analysis was performed to simulate the in situ shear tests and a test on a rock sample from the literature for comparison. The comparison shows that the failure of the sandy gravel with cobbles used in the test method did not follow the failure mode indicated in the Chinese Code or that of rocks. Instead, the failure of the sandy gravel at the site was caused by bearing-capacity failure rather than direct shear failure. The Meyerhof bearing-capacity theory [20] was used to back analyse the friction angle of the soil.

## 2 Description of Site

The test site is located in Luoyang, which is approximately 50 km south of the Yellow River, as shown in Fig. 1. Alluvial-diluvial plains formed during historic flooding of the rivers, with a thick layer of alluvial materials. The terrain is relatively flat, and the natural ground surface is between 146.7 m and 148.2 m above sea level. As part of the Luoyang subway Line 1 project, one pit was excavated for the Control Centre Subway Station. The geological profile of the site is shown in Fig. 2. A thick ( $\sim 20$  m) layer of sandy gravel with cobble was found approximately 6 m below the ground surface. The pit was approximately

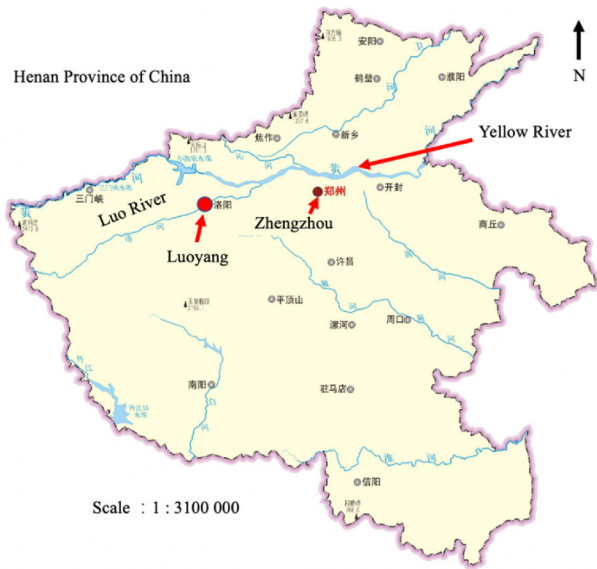


Fig. 1 Location of in situ test

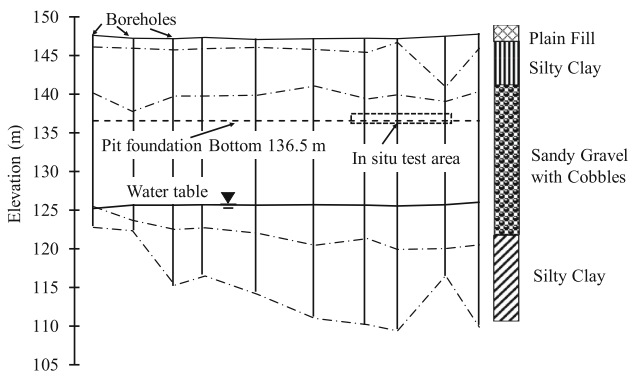


Fig. 2 Ground profile of the site

10 m deep below the ground surface. The base of the excavation was located in this layer. Therefore, the sandy gravel layer had a great impact on excavation performance. The water table at the site was approximately 22 m below the ground surface, which was well below the depth of concern.

Several large-scale direct shear tests and dynamic cone penetration (DCP) tests were performed at the site to determine the shear strength parameters of the sandy gravel at the base of the pit. Six in situ shear tests were performed in the sandy gravel layer, 10 m below the ground surface, at the base of the excavation, as shown in Fig. 2. The soil to be tested was brown and grey in colour. The in situ density of the soil was  $2200 \text{ kg/m}^3$ , indicating that the soil was in a moderately dense to dense state. The cobbles were rounded and consisted mainly of limestone, sandstone, and quartzite, as shown in Fig. 3. The particle size distributions of the six sheared samples are shown in Fig. 4. Some variation could be observed in the particle grading of the



Fig. 3 Exposure of in situ soil columns

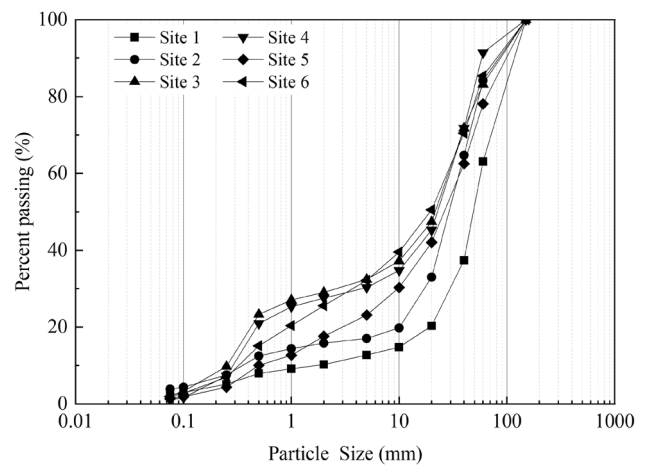


Fig. 4 Particle size distributions of the soil samples

samples. Most samples contained approximately 15 to 40% cobble. The grading parameters are listed in Table 1. The soil can be classified as sandy gravel with cobbles [21]. The moisture content of the soils at the test sites ranged from 3.04 to 5.78%, with an average value of 3.92%. DCP was

Table 1 Grading properties of the soils at the shear test site

Grading parameters	Test site 1	Test site 2	Test site 3	Test site 4	Test site 5	Test site 6
$d_{60}$ (mm)	58	37	30	30	36	30
$d_{10}$ (mm)	2	0.35	0.25	0.3	0.5	0.35
$d_{30}$ (mm)	32	18	3	5	10	4
$c_u$	29.0	105.7	120.0	100.0	72.0	57.1
$c_c$	8.8	25.0	1.2	2.8	5.6	2.3

$c_u$  coefficient of uniformity,  $c_c$  coefficient of curvature

performed at the site using a 74 mm diameter cone with a 60° cone tip, driven by a 120 kg hammer with a free fall height of 100 cm. The results showed that for 10 cm of penetration, the corrected number of drops was  $N_{120} = 22.9$ .

### 3 In Situ Direct Shear Test Procedure

In situ direct shear tests were performed per the specifications for field shear tests commonly used in China [22]. A diagram of the setup is shown in Fig. 5. Unlike normal shear box setups, which include a top and a bottom shear box, the setup in situ has only one shear box made of a 0.5 m cubic-shaped hollow steel column to provide confinement to the soil. The lower part of the soil is confined by the foundation soil, as shown in Fig. 5. A vertical load is applied on the top surface of the soil column confined in the steel column via a loading plate, and the column is sheared laterally to measure the resistance of the soil. This setup is similar to that used for in situ tests of rocks [23].

To form one soil sample, a 2.5 m long  $\times$  3 m wide  $\times$  0.8 m deep test pit was excavated at the base of the excavation to form a soil column (1 m long  $\times$  1 m wide  $\times$  0.8 m tall) at the centre of the test pit. The soil column was carefully shaped to fit into the steel column. The top surface of the soil column was flattened, and the voids were filled with fine sand to ensure the even distribution of loading from the load plate. Loading was applied via two square steel plates with a thickness of 3 cm and a width of 49 cm wide; these steel plates were placed on the

soil surface, with eight roller steel bars (49 cm long, 3 cm diameter) sandwiched between the two plates.

A 2 m long  $\times$  0.5 m wide  $\times$  0.8 m high concrete beam was placed on one side of the pit as the reaction beam for horizontal loading. A 3 cm thick steel plate (70 cm  $\times$  50 cm) was fixed on the inner side of the beam as the footing of the lateral loading jack. Steel beams and concrete blocks were used to provide reaction forces for vertical loading. Four linear variable displacement transducers (LVDTs) were installed on the four corners of the loading plate, and four LVDTs were installed on the other side of the shear box to measure vertical and lateral movement, respectively. Figure 6 shows photos of the test system. The vertical and lateral loadings were applied using hydraulic jacks. The tests used six vertical loading levels: 12.5 kN, 25 kN, 50 kN, 75 kN, 100 kN, and 150 kN. The vertical and horizontal loadings were applied as per Chinese Standard recommendations [24].

### 4 Test Results and Discussion

Figure 7 shows the load–displacement curves of the samples under shear. The positive displacements in Fig. 7b indicate downwards movement. The shear displacement curves of the samples show that the samples behave similarly to those of medium-density sand. The nearly linear relationship between the normal stress and shear stress at failure shown in Fig. 8 indicates that the friction angle ( $\phi$ ) of the soil is approximately 26.7° (assuming that the cohesion is zero), as calculated using Eq. (1):

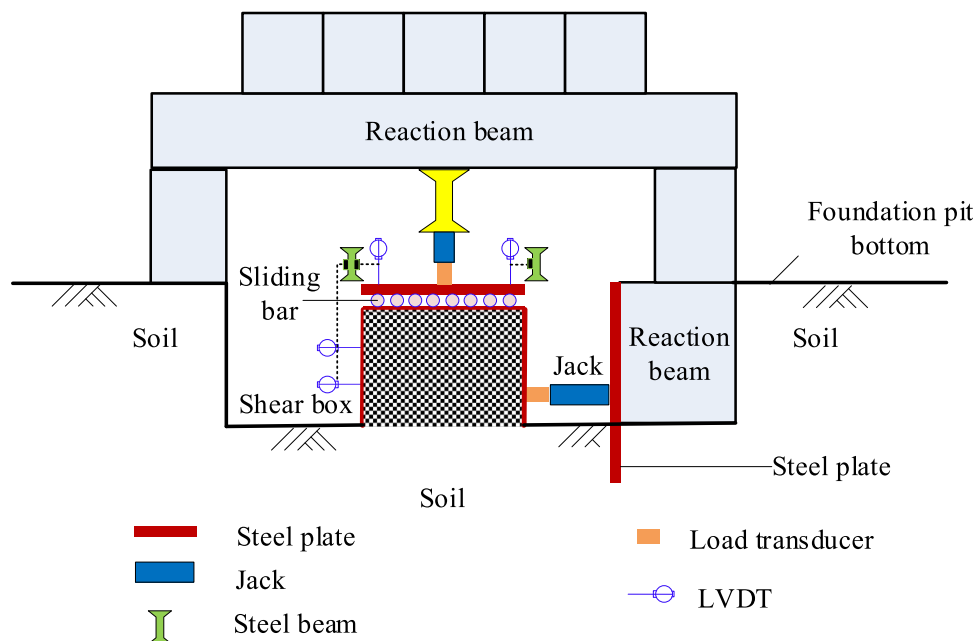


Fig. 5 Diagram of the test setup





Fig. 6 Test setup for the in situ large-scale direct shear test

$$\tan \phi = \tau / \sigma = F / N \tag{1}$$

where  $\sigma$  is the normal stress,  $\tau$  is the shear stress,  $N$  is the vertical load, and  $F$  is the horizontal load.

The strength parameters of the gravel can also be estimated based on the DCP results.  $N_{120}$  is used to calculate  $N_{63.5}$  (the number of drops for 63.5 kg of the hammer dropping from 76 cm high to penetrate 10 cm) [25, 26]:

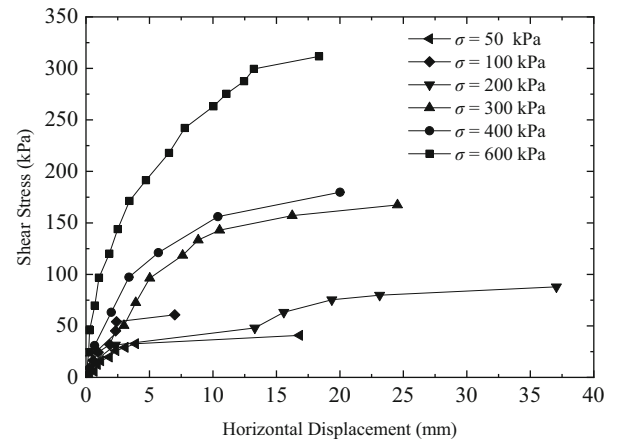
$$N_{63.5} = 3N_{120} - 0.5 \tag{2}$$

This gives  $N_{63.5} = 68.2$  using  $N_{120} = 22.9$ . The friction angle of the material should be greater than  $48^\circ$ ; this value is much greater than the value obtained based on in situ direct shear tests [27].

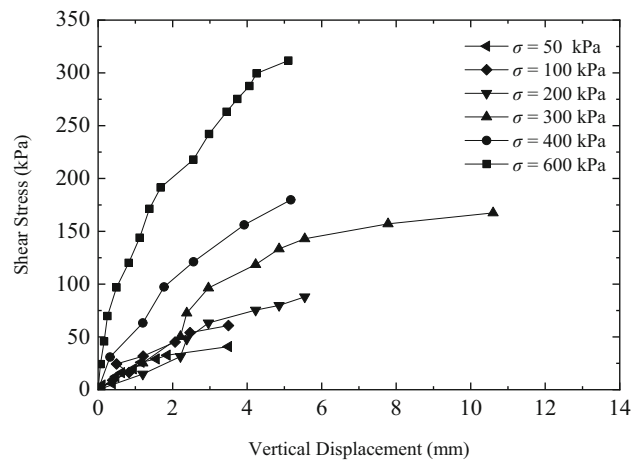
Carter suggested that the friction angle of well-graded sand-gravel mixtures should be greater than  $38^\circ$  [28]. The friction angle of soils can be obtained using the following empirical formula [29]:

$$\phi = 36 + \phi_1 + \phi_2 + \phi_3 + \phi_4 \tag{3}$$

where  $\phi_1$ ,  $\phi_2$ ,  $\phi_3$ , and  $\phi_4$  are empirical parameters affected by the soil type, relative density, soil gradation, and particle shape, respectively. Based on the characteristics of the soil tested at the site,  $1^\circ$  (gravel + sand),  $6^\circ$  (very dense,  $0^\circ$  (medium), and  $-3^\circ$  (subrounded) were used for  $\phi_1$ ,  $\phi_2$ ,  $\phi_3$ , and  $\phi_4$ , respectively, in the test soil [29]. According to this method, the friction angle of the soil at the site should be  $40^\circ$ ; this value is also much greater than that obtained from Fig. 8.



(a)



(b)

Fig. 7 Shear displacement curve. a Horizontal displacement and b vertical displacement

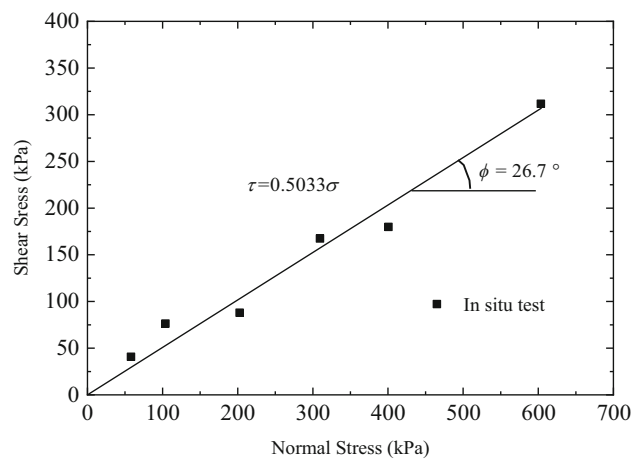


Fig. 8 Normal stress vs. shear stress curve

## 5 Failure Mechanism Analysis Using the Finite Difference Method

The above discussion indicates that the applicability of the in situ direct shear test can be problematic in certain scenarios. For some in situ tests, the shear force location may generate momentum along the shear surface [17, 30–32]. Additionally, due to the lack of a bottom shear box, the shear surface may not follow the predefined conditions at the interface of the upper and lower shear boxes used in normal shear tests. However, Eq. (1) is used in practise, as recommended in the Chinese Code [24].

Finite difference analyses were performed using a finite difference method in FLAC3D (FLAC3D, 2018) to study the discrepancy between the friction angles obtained from the empirical methods and the direct shear test results. Considering the symmetrical nature of the shear box, a half model was built for the numerical analysis, as shown in Fig. 9. In the figure,  $L$  is the width of the shear box, which is 0.5 m, and  $H$  is the height of the shear box. The ground is surrounded by horizontal constraints on three sides except for the right face for the symmetry boundary, whilst the shear box experiences vertical constraints at its base. The size of the shear box was 0.5 m  $\times$  0.5 m  $\times$  0.35 m, and the box was modelled as rigid walls. A total of 122,040 elements were generated in the model. A friction angle of 48° was assumed for the soil with a cohesion of 1 kPa to avoid numerical instability. Four in situ direct shear tests were simulated with the finite difference model, except for the case with 200 kPa of normal loading, where the horizontal load–displacement behaviour was clearly abnormal. The

Young's modulus of the soil was calculated using  $E = 25(p/p_a)^{0.5}$  MPa as recommended by Jiang et al. [33] and Oztoprak and Bolton [34]; here,  $p$  is the normal loading applied and  $p_a$  is the atmospheric pressure of 100 kPa. The dilation angle was assumed to be 19° and calculated using the method recommended by Bolton [35] for sand with a postulated critical state friction angle of 33°.

For comparison, a test on a rock sample [36] was also simulated to compare the applicability of in situ rock test methods [23] to rock samples. Considering the symmetry of the model, to enhance computational efficiency, only half of the model was constructed and analysed, with a symmetry boundary set at the centre of the model. The ground was 10  $L$  ( $L$  is the length of the sample) in length and 5  $L$  in width and depth. The ground was surrounded by horizontal constraints on three sides except for the right face for the symmetry boundary, and the ground experienced vertical constraints at its base. A test under a normal load of 433 kPa was modelled. The cohesion and friction angle of the rock obtained from the shear tests were 423 kPa and 52°, respectively [36]. The values were used in the numerical modelling with an assumed Young's modulus of 600 MPa and a Poisson's ratio of 0.25. Mohr–Coulomb failure criteria were used for both the soil and the rock in the analyses.

Figures 10 and 11 compare the shear displacement curves of the soil and the rock obtained from in situ tests with those from the numerical analyses. With the assumed soil friction angle, which is almost twice that of the value calculated with Eq. (1), the results from the numerical analysis compare quite well with the in situ test results. This indicates that Eq. (1) cannot be used to obtain soil shear strength parameters with the test method used at the site but is suitable for the rock tested [36].

To further explain the discrepancy between the performance of the test on rock and soil, the failure plane observed in the numerical simulations is presented in Fig. 12. For the rock sample, the shear plane is along the base of the shear box (Fig. 12b). For the soil sample, the shear failure (Fig. 12a) occurs deep in the ground rather than along the base of the shear box. The shear surface in the soil is similar to that of bearing-capacity failures of shallow foundations [37]; this type of failure is different from the shear failure mechanism observed in soil cracking box direct shear tests and rock in situ shear tests [23]. Therefore, the friction angle obtained using Eq. (1) would be lower than expected since the incorrect failure mechanism was used.

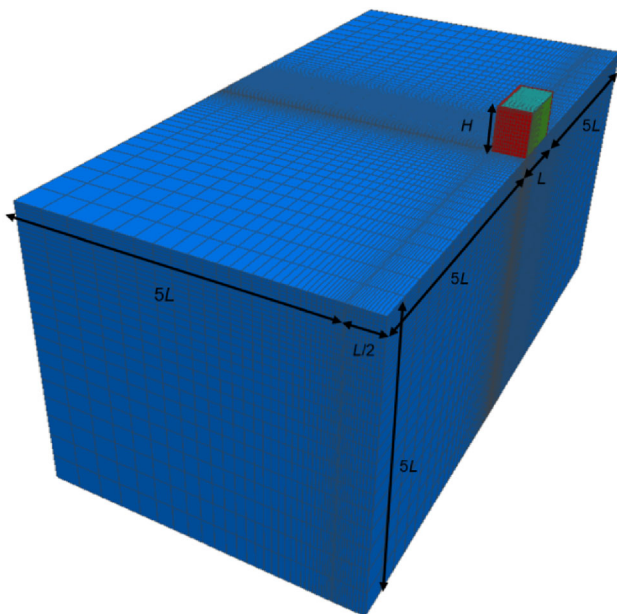
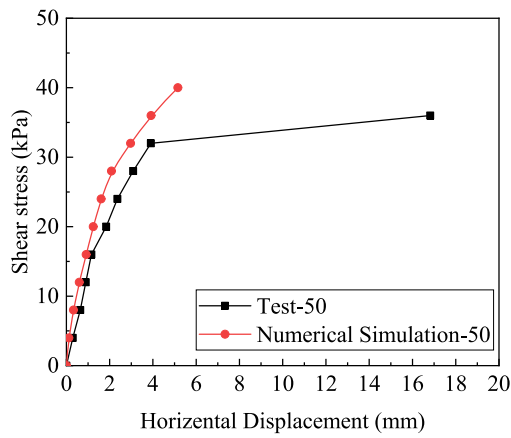
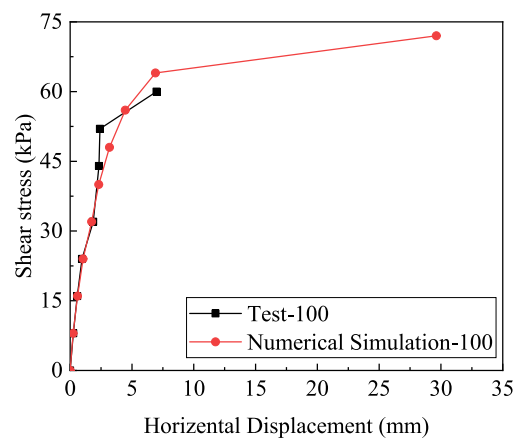


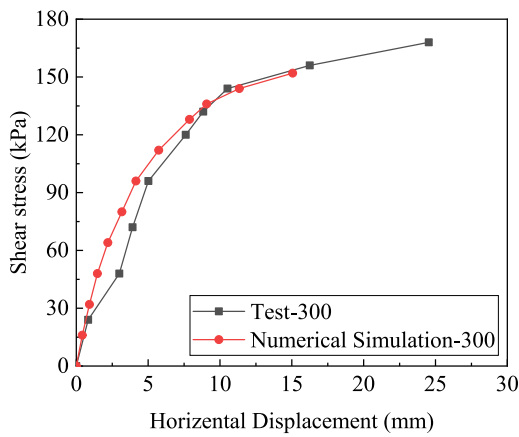
Fig. 9 Finite difference model (half model) of the in situ shear tests



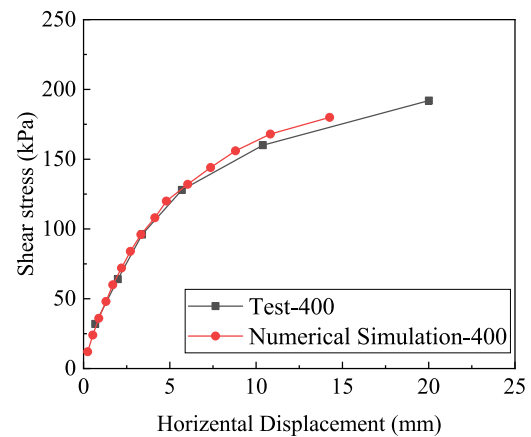
(a) 50 kPa



(b) 100 kPa



(c) 300 kPa



(d) 400 kPa

Fig. 10 Shear displacement curve of sandy gravel with cobbles obtained via in situ tests and numerical modelling

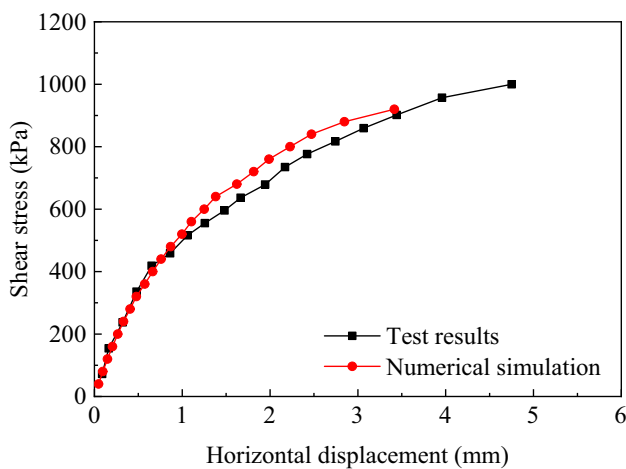


Fig. 11 Shear displacement curve of the rock specimens tested by Xing et al. [36]

## 6 Back Analysis Using the Meyerhof Equation

Based on the previous numerical analysis, the shear box enclosed soil can be considered a shallow foundation under an inclined load. Therefore, the failure of the shear tests performed at the site is a bearing-capacity failure rather than a direct shear failure. There are many methods available for calculating the bearing capacity of shallow foundations under inclined loads [20, 38, 39], and the following equation is used to back analyse the friction of the soil tested at the site:

$$q_{ult} = cN_c d_c i_c + \bar{q}N_q d_q i_q + 0.5\gamma B' N_\gamma d_\gamma i_\gamma \quad (4)$$

where the following terms are defined as follows:

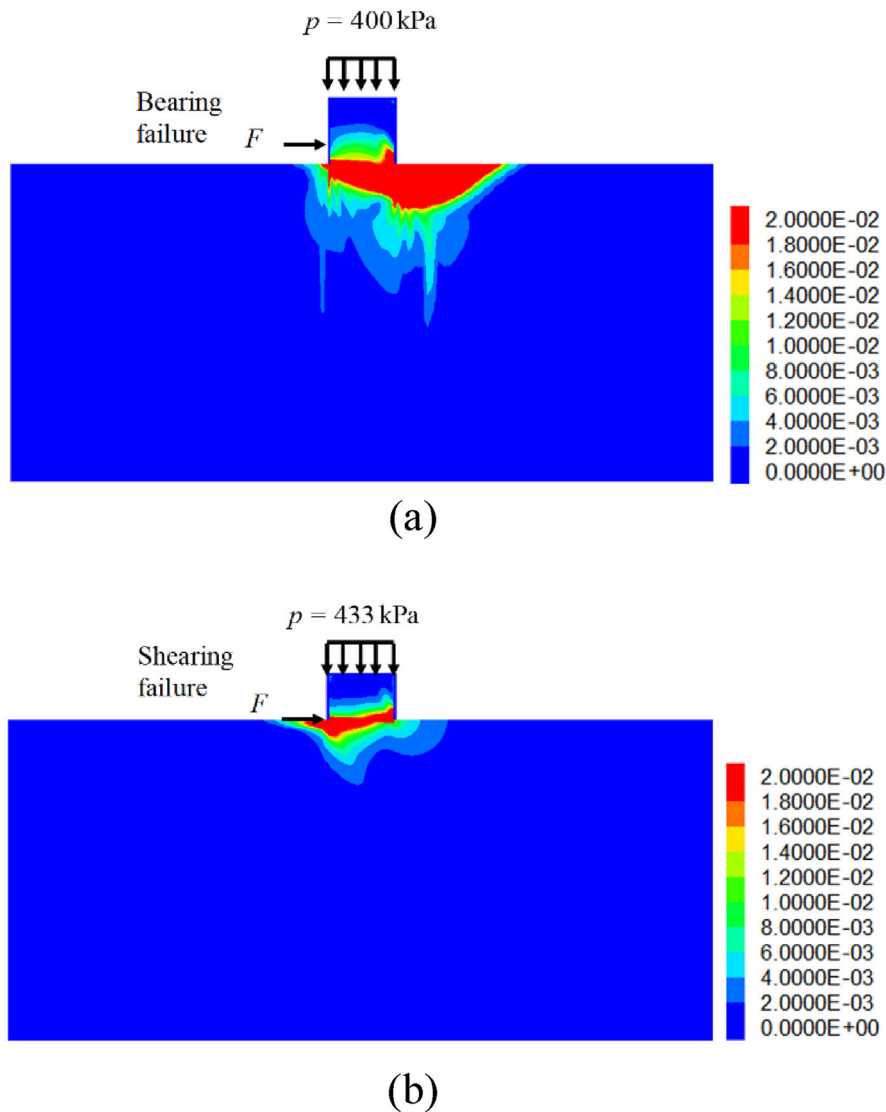


**Fig. 12** Shear strain contours on the plane of symmetry for direct shear tests on (a) sandy gravel with cobbles sample and (b) rock reported in Xing et al.

$$N_q = e^{\pi \tan \phi} \tan^2 \left( 45 + \frac{\phi}{2} \right) \quad (5)$$

$$N_c = (N_q - 1) \cot \phi \quad (6)$$

$$N_\gamma = (N_q - 1) \tan(1.4\phi) \quad (7)$$

As the shear box is square shaped and sitting on the ground surface, the shape factors ( $s_c$ ,  $s_q$ ,  $s_\gamma$ ), depth factors ( $d_c$ ,  $d_q$ ,  $d_\gamma$ ), and inclination factors ( $i_c$ ,  $i_q$ ,  $i_\gamma$ ) can be derived using the following [20, 40]:

$$s_c = 1 + 0.2 \tan^2(45 + \phi/2) \quad (8)$$

$$s_q = s_\gamma = 1 + 0.1 \tan^2(45 + \phi/2) \text{ for } \phi > 10^\circ \quad (9)$$

$$d_c = d_q = d_\gamma = 1 \quad (10)$$

$$i_c = i_q = \left( 1 - \frac{\theta^\circ}{90^\circ} \right)^2; \quad i_\gamma = \left( 1 - \frac{\theta^\circ}{\phi^\circ} \right)^2 \quad (11)$$

where  $\theta$  is the angle between vertical and horizontal loading and  $B$  is the footing width and is considered to be 0.5 m. Under inclined loading, the effective footing width  $B'$  can be derived as follows [40]:

$$B' = B - 2 \frac{F \cdot h}{N} \quad (12)$$

In this test, the shear force is applied at 0.1 m above the ground, and  $h = 0.1$  m; hence, the following is obtained:



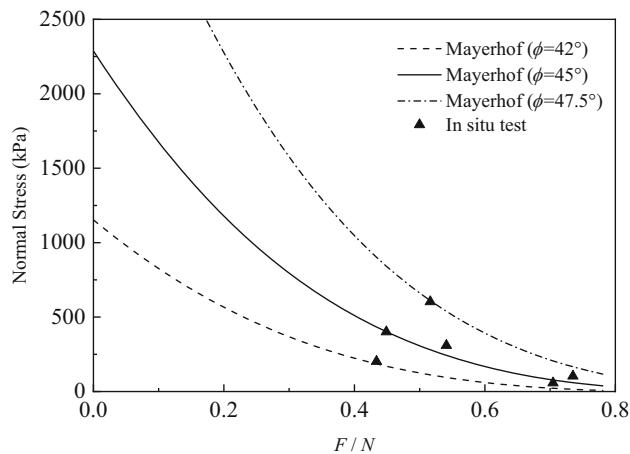


**Fig. 13**  $F/N$  vs. normal stress obtained from Meyerhof bearing-capacity theory

$$B' = B - 0.2 \frac{F}{N} = B - 0.2 \tan(\theta) \quad (13)$$

In the back analysis for this in situ test, the cohesion  $c$  and foundation depth were set to zero, the width and length of the plate were both 0.5 m, and the weight of the sandy gravel with cobbles was 22 kN/m<sup>3</sup>. The variation in  $F/N$  with  $N$  for different soil friction angles is plotted in Fig. 13, along with the in situ shear test results. Based on the bearing-capacity theory, the friction angle of the soil was within the range of 42° to 47.5°, which was close to the values obtained from the empirical methods, DCP tests, and the value used in the finite difference analysis discussed earlier. This again confirmed that the test results obtained from the shear tests could not be analysed directly using the direct shear theory described in Eq. 1. Therefore, back analysis is recommended using the bearing-capacity theory of shallow foundations to obtain the shear strength of the soil.

## 7 Conclusion

A set of large-scale single box (50 cm cubic shear box) direct shear tests were performed on sandy gravel with cobbles at the base of an excavation at a metro station. The main conclusions were as follows:

Because the bottom boundary condition was not fixed during the in situ test, the friction angle of sandy gravel with cobbles obtained (26.9°) through the in situ direct shear test was much lower than the values (> 40°) obtained through empirical equations and the value (48°) derived from in situ DCPs and finite difference analysis.

Compared with the rock direct shear test, the failure of the sandy gravel with cobbles during the in situ direct shear test did not occur along the base of the shear box, as

observed in the rock sample, but it did occur at the bottom of the sample due to the bearing-capacity failure.

The test results were back-analysed using the Meyerhof bearing-capacity equation. The analysis indicated that the direct shear test results obtained at the site could not be analysed using the direct shear failure mechanism without a fixed bottom. Therefore, back analysis using bearing-capacity theory is recommended for obtaining the soil strength parameters when a single box large shear test is performed on this type of soil.

**Acknowledgements** The manuscript was written when Junwei Jin was a visiting scholar at the UNSW Canberra. The support received from UNSW Canberra is acknowledged.

**Funding** This study received financial support from the Science and Technology Project of Henan Province (232102241011, 202102310586), Science and Technology Project of Housing Urban-Rural Development of Henan Province of China (K-1940).

**Data availability** The data of this study are available from the corresponding author on reasonable request.

## References

- Tan Y, Lu Y, Xu C, Wang D (2018) Investigation on performance of a large circular pit-in-pit excavation in clay-gravel-cobble mixed strata. *Tunn Undergr Space Technol* 79:356–374. <https://doi.org/10.1016/j.tust.2018.06.023>
- Du X, Zhang P, Jin L, Lu D (2019) A multi-scale analysis method for the simulation of tunnel excavation in sandy cobble stratum. *Tunn Undergr Space Technol* 83:220–230. <https://doi.org/10.1016/j.tust.2018.09.019>
- Lamb TW, Whitman RV (1991) *Soil mechanics*. Wiley, New York
- Takada N (1993) Mikasa's direct shear apparatus, test procedures and results. *Geotech Test J* 16:314–322. <https://doi.org/10.1520/gtj10052j>
- Terzaghi K, Peck R, Mesri G (1996) *Soil mechanics in engineering practice*, 3rd edn. Wiley, New York
- Saada AS, Townsend FC (1981) *State of the art: laboratory strength testing of soils*. ASTM Spec Tech Publ. <https://doi.org/10.1520/stp28744s>
- Potts DM, Dounias GT, Vaughan PR (1987) Finite element analysis of the direct shear box test. *Geotechnique* 37:11–23. <https://doi.org/10.1680/geot.1987.37.1.11>
- Australia S (1998) *Methods of testing soils for engineering purposes, method 6.2.2: soil strength and consolidation tests: determination of the shear strength of a soil: direct shear test using a shear box*. Australian Standard, Sydney
- ASTM D3080-98 (1998) *Standard test method for direct shear test of soils under consolidated drained conditions*, ASTM International, West Conshohocken, PA
- Jewell RA, Worth CP (1989) Direct shear tests on sand. *Geotechnique* 39(2):309–322. <https://doi.org/10.1680/geot.1989.39.2.309>
- Q181C (2020) *Effective angle of internal friction at constant volume conditions for granular materials*. Department of Transportation and Main Roads, Queensland

12. Bauer GE, Zhao Y (1993) Shear strength tests for coarse granular backfill and reinforced soils. *Geotech Test J* 16:115–121. <https://doi.org/10.1520/gtj10274j>
13. Biabani MM, Indraratna B, Nimbalkar S (2016) Assessment of interface shear behaviour of sub-ballast with geosynthetics by large-scale direct shear test. *Proc Eng* 143:1007–1015. <https://doi.org/10.1016/j.proeng.2016.06.094>
14. De Guzman EMB, Stafford D, Alfaro MC, Doré G, Arenson LU (2018) Large-scale direct shear testing of compacted frozen soil under freezing and thawing conditions. *Cold Reg Sci Technol* 151:138–147. <https://doi.org/10.1016/j.coldregions.2018.03.011>
15. Xu D, Liu H, Rui R, Gao Y (2019) Cyclic and postcyclic simple shear behavior of binary sand-gravel mixtures with various gravel contents. *Soil Dyn Earthq Eng* 123:230–241. <https://doi.org/10.1016/j.soildyn.2019.04.030>
16. Nakao T, Fityus S (2008) Direct shear testing of a marginal material using a large shear box. *Geotech Test J* 31(5):393–403
17. Matsuoka H, Liu S, Sun D, Nishikata U (2001) Development of a new in-situ direct shear test. *Geotech Test J* 24:92–102
18. Wang J, Yang Y, Chai H (2016) Strength of a roller compacted rockfill sandstone from in-situ direct shear test. *Soil Mech Found Eng* 53:30–34. <https://doi.org/10.1007/s11204-016-9360-1>
19. Xu W, Xu Q, Hu R (2011) Study on the shear strength of soil-rock mixture by large scale direct shear test. *Int J Rock Mech Min Sci* 48(8):1235–1247. <https://doi.org/10.1016/j.ijrmmms.2011.09.018>
20. Meyerhof GG (1953) The bearing capacity of foundations under eccentric and inclined loads. *Proc 3rd Int Conf Soil Mech Found Eng* 1: 440–445
21. ASTM D2487-17 (2020) Standard practice for classification of soils for engineering purposes (Unified Soil Classification System), ASTM International, West Conshohocken, PA
22. HG/T20693-2006 (2006) Specification for field direct shear test of rock and soil mass. China Planning Press, Beijing (**in Chinese**)
23. ASTM D4554-12 (2021) Standard test method for in situ determination of direct shear strength of rock discontinuities. ASTM International, West Conshohocken, PA
24. DB51/T5026-2001 (2001) Code for design of building foundation in Chengdu, Southwest Jiaotong University Press, Chengdu (**in Chinese**)
25. TB10018-2018 (2018) Code for in-situ testing of railway engineering geology. China railway Press, Beijing (**in Chinese**)
26. GB/T50480-2008 (2008) Code for in situ tests of geotechnical engineering investigation of metallurgical industry. China Architecture & Building Press, Beijing (**in Chinese**)
27. DB21/T907 (2015) Technical code for building foundation of Liaoning province. Liaoning construction design and research institute. Liaoning science and technology press, Shenyang (**in Chinese**)
28. Carter M, Bentley SP (2016) Soil properties and their correlations. Wiley, Boca Raton, FL
29. Brinch Hansen J, Lundgren H (1958) *Geoteknik*. Teknisk Forlag, Copenhagen
30. Zeigler TW (1972) In situ tests for the determination of rock mass shear strength. US army engineer waterways experiment station, Mississippi
31. Hua J, Zheng J (2017) *Geological engineering handbook*. China Architecture Publishing, Beijing (**in Chinese**)
32. Liu S (2009) Application of in situ direct shear device to shear strength measurement of rockfill materials. *Water Sci Eng* 2(3):48–57. <https://doi.org/10.3882/j.issn.1674-2370.2009.03.005>
33. Jiang G, Fumio T, Alessandro F, Junichi K (1997) Inherent and stress-state-induced anisotropy in very small strain stiffness of a sandy gravel. *Géotechnique* 47(3):509–521
34. Oztoprak S, Bolton MD (2013) Stiffness of sands through a laboratory test database. *Géotechnique* 63(1):54–70
35. Bolton MD (1986) The strength and dilatancy of sands. *Géotechnique* 36(1):65–78
36. Xing H, Liu Z, Li Q, Xu C (2007) Field shear test and analysis of rocks of the western route project for South-to-North water transfer. *Rock Soil Mech* 28(s1):69–73 (**in Chinese**)
37. Bolton MD, Lau CK (1993) Vertical bearing capacity factors for circular and strip footings on Mohr-Coulomb soil. *Can Geotech J* 30(6):1024–1033. <https://doi.org/10.1139/t93-099>
38. Viscic AS (1973) Analysis of ultimate loads of shallow foundations: closure of discussion of original paper J. *Soil Mech. Found. Div. Jan. 1973. 1F, 6R. J. GEOTECH. ENGN. DIV. V100, N.GT8, 1974, P949–951. Int J Rock Mech Min* 11(11): A230. [https://doi.org/10.1016/0148-9062\(74\)90598-1](https://doi.org/10.1016/0148-9062(74)90598-1)
39. Hansen JB (1970) A revised and extended formula for bearing capacity, Bulletin 28. Danish Geotechnical Institute, Copenhagen
40. Bowles JE (1997) *Foundation analysis and design*, 5th edn. New York

Springer Nature or its licensor (e.g. a society or other partner) holds exclusive rights to this article under a publishing agreement with the author(s) or other rightsholder(s); author self-archiving of the accepted manuscript version of this article is solely governed by the terms of such publishing agreement and applicable law.